Colloid Polym Sci (2016) 294:1823–1832
DOI 10.1007/s00396-016-3939-y

ORIGINAL CONTRIBUTION

Chiral photosensitive side-chain liquid crystalline polymers—synthesis and characterization

Xiao-Zhi He[1] · Ye-Feng Gao[1] · Jia-Jun Zheng[1] · Xiao-Yun Li[1] · Fan-Bao Meng[1] · Jian-She Hu[1]

Received: 29 January 2016 / Revised: 12 August 2016 / Accepted: 26 August 2016 / Published online: 29 September 2016

Abstract The cholesteric polysiloxanes (P series) were obtained by reacting cholesteric monomer and phenolic hydroxyl monomer in different ratios with polysiloxanes. And then the chiral azo-containing polysiloxanes (AP series) were synthesized by esterifying P series members with the acryl acid of azo acid catalyzed by DMAP. The chemical structures and liquid crystal (LC) properties of the monomers and polymers were characterized by use of various experimental techniques such as FTIR, ^{1}H-NMR, POM, DSC, TGA, XRD and ultraviolet-visible. Experimental results proved that obtained polymers were in accordance with the molecular design. The transition temperatures of the polymers exhibited a decreasing trend as the content of the cholesteric units increased and became higher by introducing the azo mesogenic core. The temperatures at which 5 % weight loss occurred are higher than 280 °C. P_2–P_6 showed blue Grandjean textures and exhibited selective reflection in the visible light region. AP series also possessed Grandjean textures, and the colors exhibited red shift with increasing content of azo moiety. On the heating cycles, when appropriate mechanical pressure was imposed on the polymers, AP_2–AP_6 selectively reflect visible light; however, there are no reflection peaks in the UV-Vis spectrum without the stimulation of mechanical pressure. All polymers exhibit left-handed optical activity due to having the same cholesteric group. The optical rotation direction of AP changes from left to right when increasing the UV irradiation time, and the photoresponsive behaviors of AP series are also investigated.

Keywords Polymer synthesis · Properties · Optical · X-ray diffraction · Liquid crystals

Introduction

Side-chain liquid crystalline polymers (SCLCPs) are an important research topic in the fields of theoretical research and engineering application due to their unique optical properties. Functional materials can be designed and synthesized by introducing functional groups into the molecular structure of SCLCPs. Functional groups include azobenzene, spironaphthoxazine, and so on. The most commonly used photochromic moieties are azobenzene. Azobenzene-containing SCLCPs have been extensively studied in recent years because of their potential applications in the field of optical storage and optical actuators [1–9].

Azo polymers are photoresponsive materials, whose properties can exhibit significant changes when exposed by a specific optical stimulus. Under UV irradiation, the structure of azobenzene transforms from planar trans-isomer into bent cis-form; this process can be reversed by visible light irradiation or thermal relaxation [10–14].

In order to explore the correlation between the structure and photoresponsive property, many novel types of azo-SCLCPs have been designed and synthesized [15–18]. Photosensitive chiral liquid crystalline polymers (CLCPs) are an important class of optical materials due to the possibility of controlling their Bragg reflection properties with the aid of light beams [19–24]. By combining the function of chiral materials and azo polymer, the azo-CLCPs exhibit several promising properties like high photosensitivity, nonlinearity,

✉ Xiao-Zhi He
xzhe9888@hotmail.com

[1] College of Science, Northeastern University, Shen-yang 110004, People's Republic of China

easiness of molecular design, and so on, extending the possible design of next-generation optical devices and broadening the scope of applications.

Among many methods of preparing photosensitive LC polymers, the most efficient one is covalent bonding of the photoactive molecules to LC polymers. The main-chain of azo polymers can be polyacrylic acid, polymethylacrylic acid, polyurethane, polysiloxanes, etc. A main-chain of polysiloxane is preferred to others owing to its high chain flexibility, potentially enabling an easy motion of the azo side groups and favoring the recognization processes at the supermolecular level [25–39]. Due to the potential optical application, the research focuses on a larger extent on polysiloxane-based SCLCPs. One way to obtain azo polysiloxane is hydrosilylation reaction, but some azo compounds have been used as inhibitors of hydrosilylation, the reaction is difficult to perform, and the reaction time is extremely long [40]. Another reported method was firstly performed by Abe in 1995 by esterification [41]. Abe's esterification reaction can extensively avoid the azo compounds' inhibition to hydrosilylation. However, the polymers always retain a small quantity of carboxyl groups, so a new opposite idea is thought out to completely perform the esterification. At first, a precursor polymer with phenolic hydroxyl group was synthesized by hydrosilylation, then it reacted with the acryl acid of azo acid catalyzed by 4-dimethylaminopyridine (DMAP). The advantage of this synthetic method is that the excess of acryl acid can ensure the esterification completion and improve Abe's esterification, and at the same time, many different azo polysiloxane liquid crystals were synthesized and studied.

In this research, a novel cholesteric polysiloxane precursor (P series) was firstly prepared by reacting M_1 (cholesterol 4-allyloxybenzoate) and M_2 (4-hydroxyphenyl-4(allyloxy)benzoate) with polymethylhydrosiloxane, then P series polymers reacted with the acryl chloride of M_3 (6-(4-((4-nitrophenyl)diazenyl)phenoxy)-6-oxohexanoic) to obtain AP series. The mesomorphic properties of polymers were characterized by differential scanning calorimetry (DSC), polarized optical microscopy (POM), and X-ray. The structures of monomers and polymers were confirmed by FTIR and ^{1}H-NMR. The optical properties were tested by specific rotation and UV–Vis spectrum. The relationship between structures and properties was also investigated.

Experimental procedures

Materials

4-Hydroxybenzoic acid, hydroquinone, adipic acid, pyridine, dichloromethane and tetrahydrofuran, paranitroanilinum, 3-bromopropene, and cholesterol were bought from Sinopharm Chemical Reagent Co., Ltd (China). Polymethylhydrosiloxane (PMHS, M_n = 882–1062) and hexachloroplatinic acid hydrate were obtained from Jilin Chemical Industry Company (China). Toluene used in the hydrosilylation reaction was first refluxed over sodium and then distilled under nitrogen. All other solvents and regents were purified by standard methods.

Measurement

IR spectra were measured by a PerkinElmer Spectrum One FT-IR spectrometer (PerkinElmer Instruments, USA). ^{1}H-NMR spectra (400 MHz) were recorded on a Bruker AV 400 spectrometer in 5-mm o.d. sample tubes. Specific rotation was performed with a PerkinElmer 341 polarimeter. All optical activity measurements of P series and AP series were performed in tetrahydrofuran (THF) with a Na lamp (λ = 589 nm). Ultraviolet–visible spectrophotometry was measured by a PerkinElmer Lambda 950 instrument.

Phase transition temperatures and thermodynamic parameters were determined by using a Netzsch DSC 204 (Netzsch, Germany) with a liquid nitrogen cooling system. The heating and cooling rates were 10 °C min^{-1}. A Leica DMRX (Leica, Germany) polarizing optical microscope equipped with a Linkam THMSE-600 (Linkam, UK) hot stage was used. XRD measurements were performed with a nickel-filtered Cu-Kα radiation (λ = 0.1542 nm) with a DMAX-3A Rigaku (Rigaku, Japan) powder diffractometer.

Synthesis

Synthesis of the monomers

Synthesis of M_1 and M_2 Cholesterol (4-allyloxybenzoate) (M_1) was synthesized with similar ways according to previous reports [10]: Yield 86 %, mp 113.2 °C, $[\alpha]_{589}^{18.0} = -5.45°$. IR (KBr): 3082 (=CH), 2951, 2850 (–CH_3, –CH_2), 1711 (C=O), 1645 (C=C), 1605–1450 (Ar–), 1258 cm^{-1} (C–O–C). ^{1}H-NMR ($CHCl_3$, δ, ppm): 0.68–2.45, 3.56, 5.45 (m, 45H, cholesterol-H), 4.57–4.60 (d, 2H, CH_2=CHC$\underline{H}_2$), 5.29–5.39 (m, 2H, C$\underline{H}_2$=CH), 6.04–6.11 (m, 1H, CH_2=C$\underline{H}$), 6.90–8.00 (m, 4H, Ar–H).

4-Hydroxyphenyl-4(allyloxy) benzoate (M_2) was synthesized with similar ways according to previous reports [10]. Yield 82 %, mp 119 °C. IR (KBr): 3650–3250 (–OH), 2951, 2850 (–CH_2), 1748 (C=O), 1647 (C=C), 1605–1429 (Ar–), 1245 cm^{-1} (C–O–C). ^{1}H-NMR ($CHCl_3$, δ, ppm): 4.52–4.58 (d, 2H, CH_2=CHC$\underline{H}_2$), 5.25–5.40 (m, 2H, C$\underline{H}_2$=CH), 6.01–6.13 (m, 1H, CH_2=C$\underline{H}$), 7.20–8.15 (m, 4H, Ar–$\underline{H}$).

Synthesis of M_3 and B The synthetic route of 6-(4-((4-nitrophenyl)diazenyl)phenoxy)-6-oxohexanoic acid (M_3) is shown in Scheme 1. Fifty milliliters of $NaNO_2$ solution (0.0656 g mL^{-1}) was dropped into 40 mL of hydrochloric acid (6 mol L^{-1}) containing 40 mmol para-nitroanilinum under ice-water bath. After stirring for 0.5 h, urea was gradually added into the above solution; the process was monitored with potassium iodide starch test paper. The

Scheme 1 The synthetic routes of M_3 and B

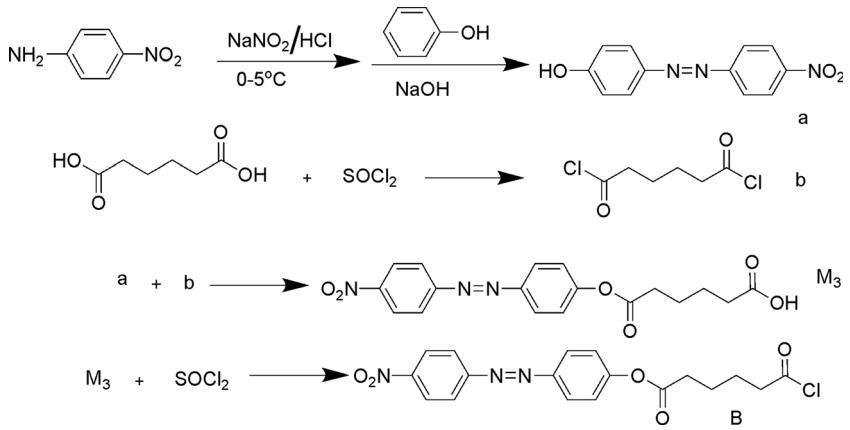

process did not stop until the test paper became blue. Then, 50 mL of phenol solution (0.0776 g/mL) was dropped into the above solution. The pH value was controlled within 9–10 by using 10 % NaOH solution, and the solution was stirred for 2 h. The reaction mixture was precipitated in hydrochloric acid aqueous solution. The resulting precipitate was washed by water and recrystallized from ethanol-water to obtain 4-((4-

Scheme 2 The synthetic route of P and AP series and schematic illustration of selective reflection

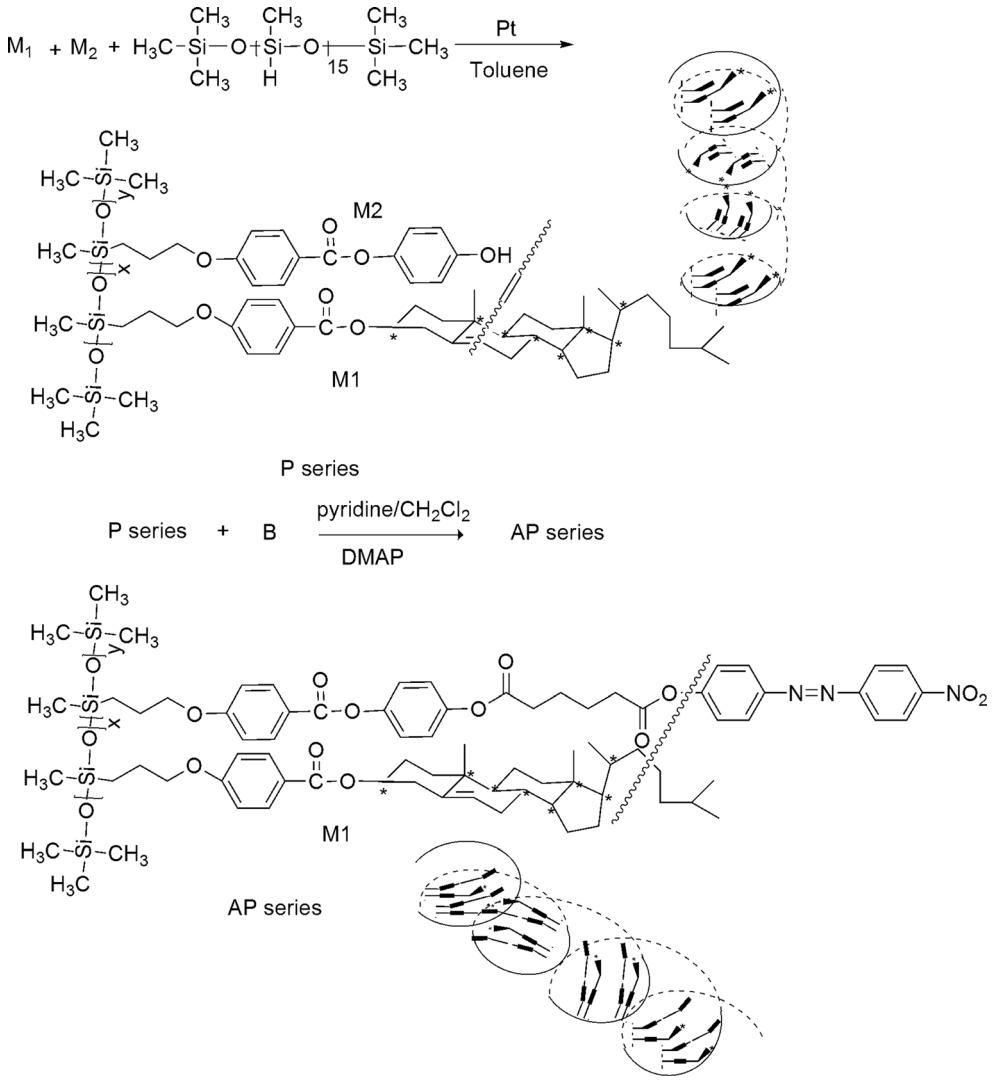

Table 1 The feed ratio of P and AP series

Sample	Feed					Feed		
P series	PMHS (mmol)	M_1 (mmol)	M_2 (mmol)	$M_1/(M_1 + M_2)$	AP series	P (g)	M_3 (g)	Yield (%)
P1	0.3000	4.2750	0.2250	5 %	AP1	0.5	0.0242	46 %
P2	0.3000	4.0500	0.4500	10 %	AP2	0.5	0.0496	52 %
P3	0.3000	3.8250	0.6750	15 %	AP3	0.5	0.0762	50 %
P4	0.3000	3.6000	0.9000	20 %	AP4	0.5	0.1042	47 %
P5	0.3000	3.1500	1.3500	30 %	AP5	0.5	0.1641	55 %
P6	0.3000	2.7000	1.8000	40 %	AP6	0.5	0.2307	51 %
P7	0.3000	2.2500	2.2500	50 %	AP7	0.5	0.3051	50 %

nitrophenyl)diazenyl)phenol as red sheet powder (yield 89 %, mp 218–219 °C).

Adipic dichloride (22.6 g, 0.12 mol, synthesized in laboratory) was dissolved in the mixture of tetrahydrofuran (100.0 mL) and pyridine (10 mL). The solution was slowly dropped into the round-bottom flask containing 5.0 g (0.1 mol) of 4-((4-nitrophenyl) diazenyl)phenol and 200 mL of tetrahydrofuran, stirred for 0.5 h at room temperature, and refluxed for 18 h, then the cold reaction mixture was precipitated into water. The crude products were washed with hot water and crystallized three times with alcohol to obtain 6-(4-((4-nitrophenyl)diazenyl) phenoxy)-6-oxohexanoic acid as red powder (yield 62 %, mp 155.5 °C). IR: 3250–2500 (–COOH), 2980, 2850 (–CH3, –CH2), 1750 (C=O), 1708 (–COOH), 1605–1450 (Ar–), 1521, 1342 (–NO2), 1403 (N=N). ^{1}H-NMR ($CDCl_3$): δ1.80–2.66 (m, 8H, –C$\underline{H}_2$–), 7.33–8.39 (m, 8H, Ar–$\underline{H}$).

The synthesis of acyl chloride of monomer M_3 was as follows. A few drops of DMF was added to a suspension of 6-(4-((4-nitrophenyl)diazenyl)phenoxy)-6-oxohexanoic acid (0.1 mol) in fleshly distilled thionyl chloride (40 mL), and the reaction mixture was refluxed for 10 h, and then the excess thionyl chloride was removed under reduced pressure to give the corresponding acid chloride (B).

Synthesis of P and AP series

The synthesis of AP series was conducted by two steps, which are outlined in Scheme 2. And the polymerizations of P series and AP series are shown in Table 1.

Synthesis of P series M_1, M_2 (in different ratio as given in Table 1), and PMHS were dissolved in anhydrous and freshly distilled toluene. The mixture was heated to 65 °C under nitrogen and anhydrous conditions, and 4 mL of tetrahydrofuran solution of hexachloroplatinate hydrate (IV) catalyst (5 mg/mL) was injected into the reaction solution with a syringe twice. The hydrosilylation reaction was completed when the infrared spectra showed no Si–H absorption peak at 2166 cm^{-1}, followed by precipitation with methanol. The products were dried in vacuum at room temperature. IR (KBr, cm^{-1}): 3500–3250 (–OH), 2980, 2850 (–CH_3, –CH2), 1735, 1711 (–C=O), 1605–1450 (Ar–), 1200–1000 cm^{-1} (Si–O–Si).

^{1}H-NMR ($CDCl_3$, δ, ppm): 0–0.20 (s, 1H, Si–C$\underline{H}_3$), 0.41–0.54 (m, 0.42H, Si–C$\underline{H}_2$–), 0.79–2.28 (m, 8.2H, alkyl-H), 3.66–4.64 (m, 0.62H, –C$\underline{H}_2$O–, –C$\underline{H}$–O–), 5.16–5.39 (m, 0.18H, ethylene-$\underline{H}$ in cholesterol), 6.71–7.89 (m, 1.11H, Ph–$\underline{H}$).

Synthesis of polymer AP series AP was synthesized by esterification of P series with acyl chloride of 6-(4-((4-nitrophenyl) diazenyl)phenoxy)-6-oxohexanoic. The synthetic routes of AP_1–AP_7 were similar, for example, the synthetic process of AP_4 is as follows: 0.5 g of precursor polymer P_4 was solved in the mixture solution of THF (80 mL) and pyridine (20 mL), then 50 mL of THF solution containing 6-(4-((4-nitrophenyl) diazenyl)phenoxy)-6-oxohexanoic acyl chloride (excess 10 % than P_4) and 0.005 g of catalyst DMAP was dropped into the above mixture solution. The reaction was refluxed for 24 h and then poured into the dilute acid solution. The crude product was washed with water and recrystallized with ethanol to obtain a faint yellow polymer (yield 40 %). IR: 2980, 2850 (–CH_3, –CH_2), 1765, 1735, 1711(–C=O), 1605–1450 (Ar–), 1527, 1344 (–NO_2), 1421 (N=N), 1200–1000 cm^{-1} (Si–O–Si). ^{1}H-NMR ($CDCl_3$, δ, ppm): 0–0.20 (s, 1H, Si–C$\underline{H}_3$), 0.41–0.54 (m, 0.42H, Si–C$\underline{H}_2$–), 0.78–2.32 (m, 9.0H, alkyl-H), 3.66–4.70 (m, 0.63H, –C$\underline{H}_2$O–, –C$\underline{H}$–O–), 5.16–5.39 (m, 0.18H, ethylene-$\underline{H}$ in cholesterol), 6.71–8.22 (m, 1.31H, Ph–$\underline{H}$).

Results and discussion

Preparation and characterization

Cholesteric liquid crystalline (M_1), monophenol moiety (M_2), and azo acid compound (M_3) were synthesized. M_1 was

prepared by esterification of cholesterol with 4-allyloxy benzoic acid chloride. M_2 was obtained by esterification of hydroquinone with 4-allyloxy benzoic acid chloride. M_3 was prepared by esterification of adipoyl chloride with 4-nitrophenyl diazenyl phenol.

The polymer P series was synthesized by a one-step hydrosilylation reaction between Si–H groups of PMHS and olefinic C=C of monomers in anhydrous toluene with hexachloroplatinate acting as a catalyst at 60 °C. The yields and properties of P series are summarized in Table 1, and the unreacted Si–H groups of all polymers were measured from ^{1}H-NMR and IR spectra. In the NMR spectra, the decrease of the peak near 4.70 ppm was followed, and the decrease of the Si–H characteristic absorption at 2166 cm^{-1} was observed during the reaction process in IR spectra. When the Si–H bond completely disappeared, the mixture was precipitated with methanol three times, then the products were dried in vacuum at room temperature.

^{1}H-NMR data and IR spectra of P series showed the disappearance of Si–H and the appearance of characteristic peaks of M_1 and M_2, suggesting that all the Si–H in PMHS was substituted via hydrosilylation action, and the monomers were connected to the polysiloxane chains successfully.

AP series were prepared by esterification of polymer P series with 6-(4-((4-nitrophenyl)diazenyl)phenoxy)-6-oxohexanoyl chloride at different ratios (10 % in excess, DMAP as catalyzer). IR spectra showed that the hydroxy peak disappeared; the characteristic bands of nitro and azo peaks appeared at about 1527, 1344, and 1421 cm^{-1}; and a new ester peak turned out at 1765 cm^{-1}. From ^{1}H-NMR, the chemical shift at 8.20 ppm further confirmed that the esterification had been completed thoroughly. The IR comparison diagram of P series and AP series is shown in Fig. 1.

Analysis of optical rotation and reflection spectra

Cholesterol is a chiral material possessing excellent rotation properties, and monomers and polymers with cholesterol also tend to have good optical properties. Cholesterol has optical chirality in $CHCl_3$, the specific rotation (SROT) of cholesterol was −33° (c = 0.4 g L^{-1}, $CHCl_3$), and the values of cholesterol 4-allyloxybenzoate (M_1) was −5.4° (c = 0.4 g L^{-1}, $CHCl_3$). M_1 has wonderful selective reflection on the heating and cooling processes. Generally, solvent, temperature, chain length, and substituent can affect the handedness of the cholesteric liquid crystals. In the present study, the P series and AP series (c = 0.4 g L^{-1}, $CHCl_3$) all exhibited optical chirality and they all showed the same handedness. From Table 2, it can be seen that the optical activity of P and AP series tended to decrease as the contents of chiral groups became smaller. Optical activity of P is higher than that of AP series due to the disturbance of rotation of chiral groups caused by the introduction of the azo group. In order to investigate the effect of the chiral group and azo cis-trans-isomerisation on the value of optical rotation of polymers, the changing trend of optical rotation was measured when the polymer solution was irradiated by UV light. Firstly, the values of optical rotation increased with irradiation time, and then the direction of optical rotation changed from left lateral to right. The results showed that the cis-trans-isomerization of the azo group affected the main-chain and induced the reversion of rotation direction. The cis-trans-isomerization of the azo group induced the azo group to move and successively drive the polymer backbone to advance, meanwhile the helical structure caused by the polymer main-chain interconverts between the right and the left spirals. The representative curves of AP1 and AP4 were shown in Fig. 2.

In the heating and cooling processes, the selective reflection of cholesteric monomers can be usually found, while for

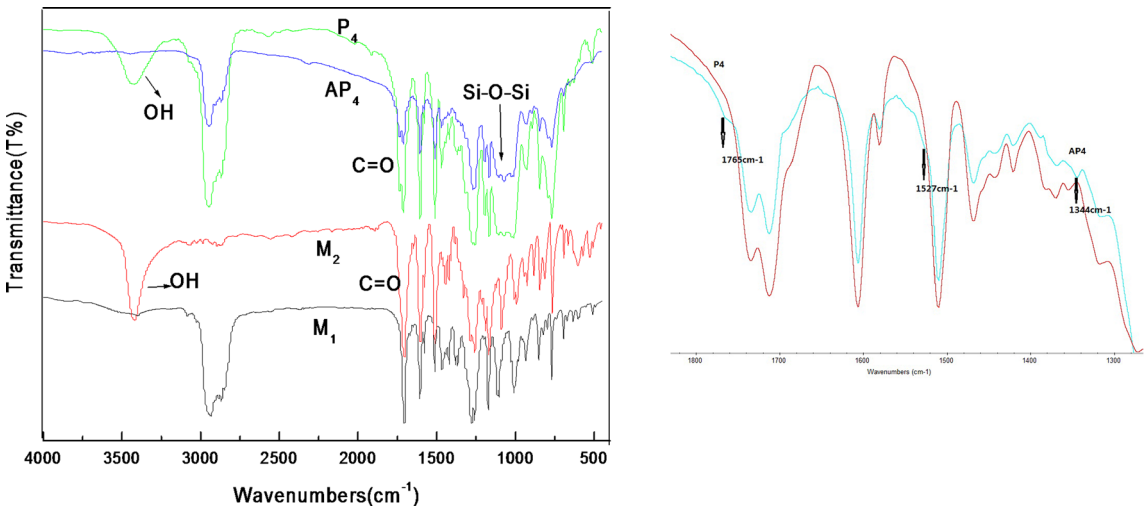

Fig. 1 The FTIR spectrum of P_4 and AP_4

Table 2 Thermal properties, specific rotation, and selective reflection of P series and AP series

P series	T_g	T_i	T_d	SR_1	SR_2	AP series	T_g	T_i	T_d	SR_1	SR_2[a]
P1	76.3	286.5	321.6	−69.59	–	AP1	64.4	267.8	319.2	−59.70	–
P2	62.0	227.3	317.1	−67.20	570	AP2	63.1	232.3	315.0	−46.20	+
P3	60.5	225.6	315.0	−59.19	570	AP3	62.4	230.1	310.5	−37.50	+
P4	60.2	221.7	312.5	−50.56	570	AP4	61.5	228.6	294.5	−35.17	+
P5	56.8	198.8	293.3	−41.17	464	AP5	61.8	199.1	290.2	−25.58	+
P6	50.6	139.9	289.6	−29.84	464	AP6	58.6	190.2	288.4	−21.06	+
P7	45.7	125.8	306.5	−22.40	–	AP7	56.1	185.0	302.7	−15.44	–

T_g glass temperature, T_i isotropic temperature, T_d temperature of the samples at 5 % loss weight, *SR1* specific rotation, *SR2* selective reflection

[a] Selective reflection can be seen when heating with pressing, cannot be found through UV–Vis spectrum

cholesteric polymer, the selective reflection cannot often be found unless the structure of polymer is in accordance with the condition of selective reflection. In this study, we found the following regulations that the selective reflection for cholesteric polymer was easy to appear when the length of the comonomer was similar with that of the cholesterol monomer.

The reflected wavelengths of P series were characterized with a PerkinElmer Lambda 950 instrument when the samples were heated to their mesophases (P_1–P_5 to 140.0 °C, P_6 and P_7 to 120 °C) without any external field. The selective reflection of P_2–P_6 can be obviously seen. The lengths of M_1 and M_2 are close and the steric hindrance of M_2 is small, so when the chiral group rotates, M_2 can well comply with the rotation, and P_2–P_6 exhibit selective reflection. From P_2 to P_4, there are absorptions at about 537 nm and P_5 and P_6 have absorptions at about 464 nm. Figure 3 shows the maximum reflected wavelength of P series. As to AP series, the length of M_3 was longer than that of M_1, so M_3 could not well comply with the rotation of cholesterol, and the selective reflection could be observed on the glass in the heating and cooling processes when pressing, but it could not be obviously observed on the UV–Vis spectrum.

Optical properties

The photoresponsive behavior of the azo-containing SCLCPs was also investigated. The UV–Vis spectra of the AP series in chloroform (c = 0.04 g L^{-1}) were recorded. The spectrum exhibited one strong absorption band around 350 nm and another weak one around 450 nm, which were typical for the azo-containing compounds and could be ascribed to the π–π* and n–π* electron transition of the –N=N– bond, respectively. The absorbance of the π–π* transition band increased

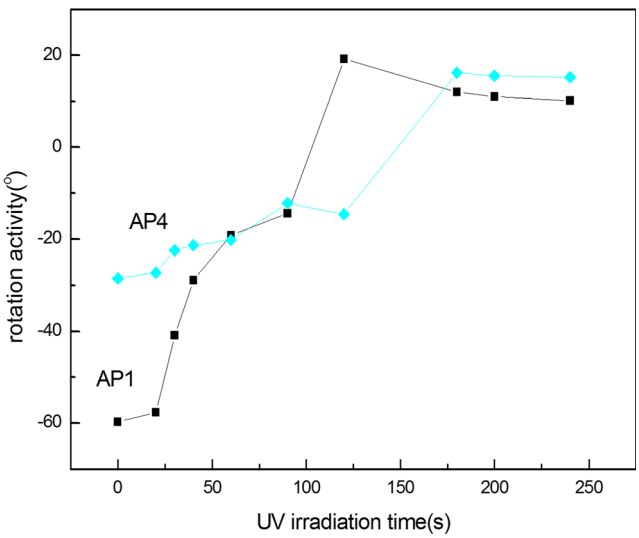

Fig. 2 The change in trend of specific rotation of AP series with UV irradiation time

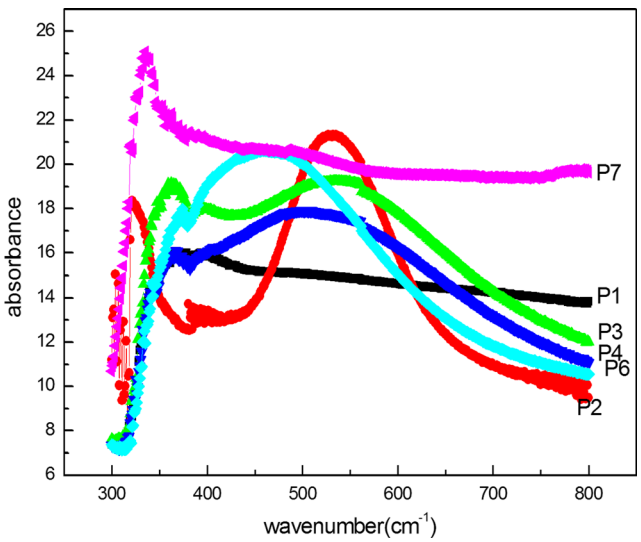

Fig. 3 Selective reflection spectra of P series

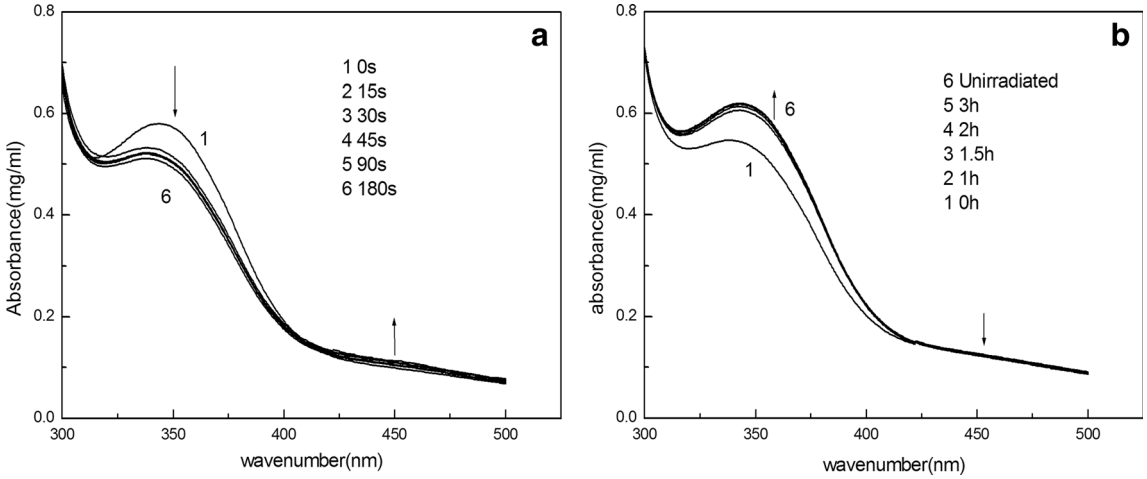

Fig. 4 UV–Vis spectral changes in dependence of time for the solution of AP_3 at 25 °C upon irradiation with 365 nm UV light (**a**) and upon irradiating the polymer solution at the photostationary state with visible light (**b**)

linearly with the increase of the contents of azo moieties, which confirmed the successful esterification of P series with the acyl chloride of M_3.

Upon irradiation with 365 nm UV light, the AP series changed from trans- form to cis- form until a photostationary state was eventually reached (Fig. 4a). Intensity of the π-π^* transition band around 350 nm decreased rapidly, whereas that of the n-π^* transition band around 450 nm slightly increased. Irradiating the thermodynamically less stable cis-isomer with visible light ($\lambda > 430$ nm) led to the cis- to trans- back-isomerization process (Fig. 4a).

Texture analysis

The POM method is essential to analyze the liquid crystal properties. It may give parameters like melting point, clearing point, changes of different LC phase and morphology of texture, and orientation defect.

During the heating cycle, for the precursor polymer, P_1~P_6 firstly showed a Grandjean texture, then P_1~P_3 showed a blue oil-streaked texture and P_4 and P_5 blue a Grandjean texture; at the same time, the selective reflection phenomenon could be seen on the glass slide, but only a Grandjean texture could be observed for P_7. All of the textures are typical textures of

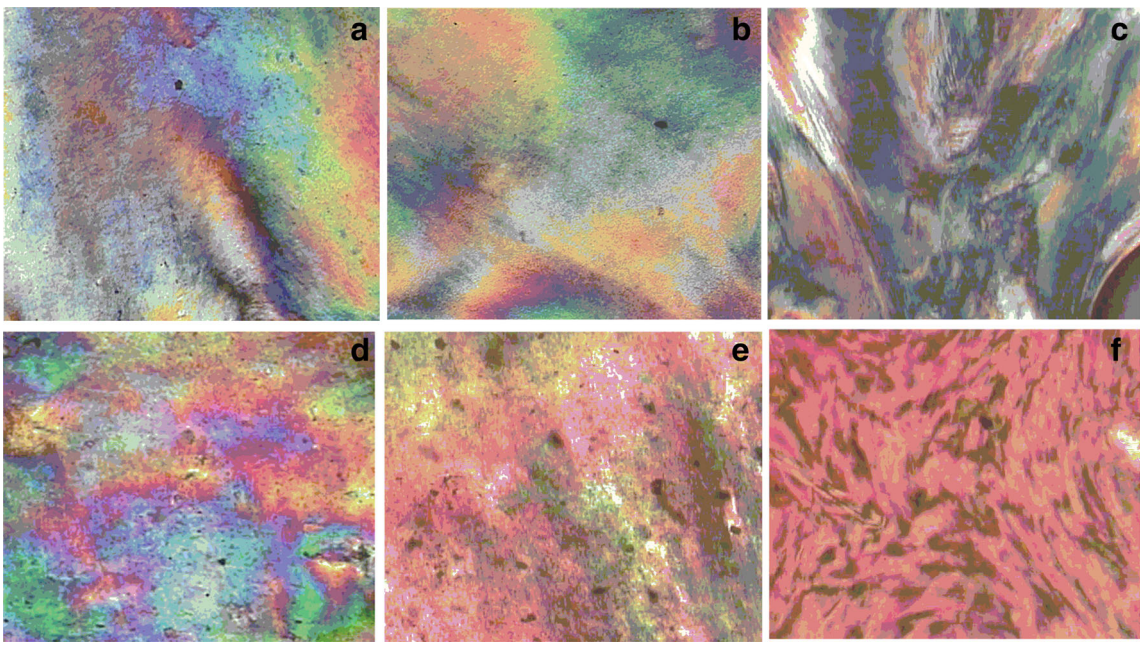

Fig. 5 Optical texture of P and AP series (×200). **a** P_1 heating to 173.3 °C. **b** P_2 heating to 197.2 °C. **c** P_4 heating to 152.3 °C. **d** AP_1 heating to 197.2 °C. **e** AP_4 heating to 134.8 °C. **f** AP_7 heating to 114.6 °C

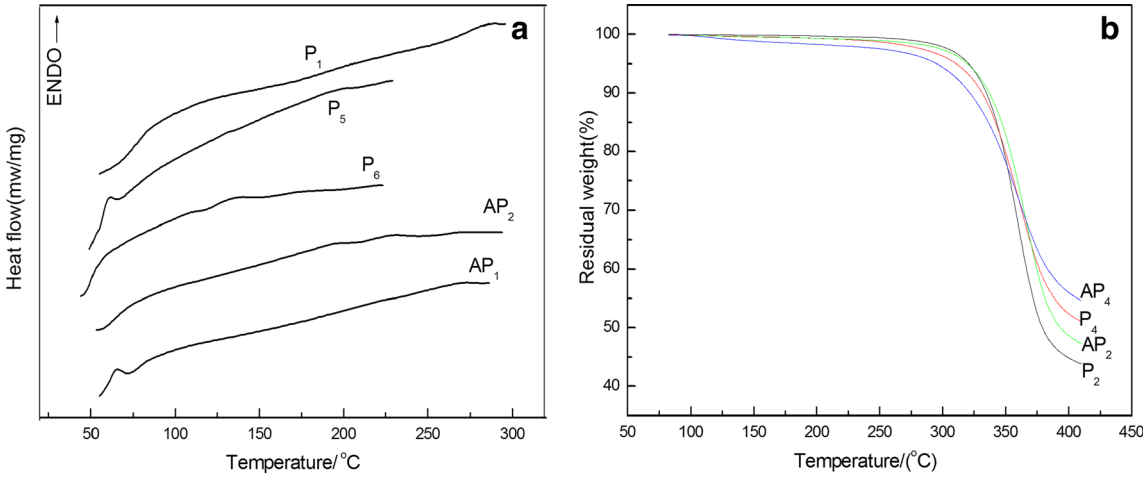

Fig. 6 DSC (**a**) and TGA (**b**) thermograms of P and AP series

cholesteric LC polymers. On the cooling cycle, a similar changing process could also be observed. The representative photographs were shown in Fig. 5a–c. The more contents the nonliquid crystalline parts have, the earlier the disappearance of the liquid crystalline phase would be. Based on the analyzed textures, the introduction of M_2 into polymer made the selective reflection phenomenon turn out easier as the result of its proper molecular length and weaker steric hindrance.

During the heating cycle, AP_1~AP_7 firstly showed a Grandjean texture and then had a rich color change, AP_1~AP_2 had a blue-green change, and AP_3~AP_7 had a red-green variety, while the red color gradually increased. This phenomenon proved that the azo component had been introduced successfully. On the cooling cycle, a similar changing process also could be observed. The representative photographs were shown in Fig. 5d–f). The liquid crystalline phase of P series and AP series could be preliminarily grouped as cholesteric phase.

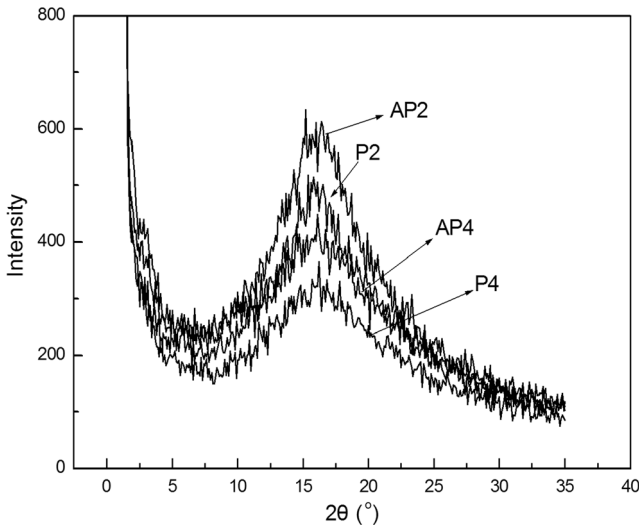

Fig. 7 X-ray profiles of representative polymers of P and AP series

Thermal analysis

The phase behavior of the LC molecule may be readily evaluated by DSC which provides an effective measurement of energy required to raise the temperature as a function of temperature. Representative DSC curves of P and AP series on the second heating scan were presented in Fig. 6a; phase transition temperatures and the results of thermal analysis were shown in Table 2. DSC curves showed a glass transition temperature (T_g) and the temperature of mesophase-isotropic phase transition (T_i). All of the transitions are reversible and did not change during repeated heating and cooling cycles. The phase transition temperatures noted in DSC thermograms were consistent with the mesomorphic transition temperatures observed by POM.

For the precursor polymer, the values of T_g and T_i tended to cut down with the decrease in content of M_1. The structure of M_1 with steroid has steric hindrance, so the decrease in content of M_1 could lower T_g values, while M_2 has no liquid crystalline properties, so the increase in content of M_2 would reduce T_i values. For the AP series, the values of T_g and T_i decreased, but still higher than those of P series, which was due to the introduction of M_3. The structure of M_3 could be divided into flexible and hardcore parts; the flexible part would decrease the T_g value and the hardcore part could increase the T_g value. The balance between two parts resulted in higher T_g values of AP series compared to those of P series. The azobenzene part of M_3 had a cis- form and a trans- form; the cis- form was bad with the orientation and led to the decrease in T_i values, while the trans- form was good with the orientation and led to the increase in T_i values. The balance between the two parts made T_i values of AP series higher than that of P series and led to the decrease in variation trend. The mesophase temperature ranges of AP series were higher too. Temperature at which 5 % weight loss occurred (T_d) was greater than 280 °C for P series and AP series, which revealed that the synthesized P

and AP series both had high thermal stability. The representative TGA curves were shown in Fig. 6b.

X-ray diffraction analysis

The LC phase of the polymers can be concluded preliminarily by DSC and POM, but it is also necessary to give more proof by XRD analysis with additional information about their structure parameters. XRD curves were measured by the method of powder XRD, and XRD patterns of representative polymers were shown in Fig. 7.

Because P and AP series own one LC phase, the XRD curve was tested around 140 °C, at which point they owned wonderful LC properties. For P and AP series, the reflection peak in the small angle did not appear, which could be concluded that the polymers did not have smectic layers, and broad peaks appeared at $2\theta \approx 15.90–16.10°$ (d = 5.57–5.49 Å). The high d values were in accordance with the regular pattern of the cholesteric polymer, which was ascribed to the rotation of the cholesteric group. Combining the POM with XRD measurements might reveal that the P and AP series were in the cholesteric phase.

Conclusions

In this study, the cholesteric azo-liquid crystalline polysiloxanes can be obtained through two steps: precursor P series were obtained first by reacting M_1, M_2, and polymethylhydrosiloxane and then esterifying P series members with acyl chloride of M_3 with DMAP as a catalyst to obtain AP series with the cholesteric phase. Combining cholesteric and azo units into a side-chain liquid crystalline polymer is hopeful to get azo-polymer with a colorful selective reflection phenomenon.

All of the obtained polymers showed that high thermal stability at which 5 % weight loss occurred was greater than 280 °C. The T_g and T_i values of P series and AP series were all at downtrend; the T_g values and T_i values of AP series were higher than those of P series, and the mesophase temperature ranges of AP series were higher too, which indicates that AP series owned better stability. P series presented a typical Grandjean texture of the cholesteric phase, selective reflection can be seen, and the absorption peak can be observed on the UV–Vis spectrum. AP series showed a Grandjean texture too, and the texture color turned to red with the increase in contents of the azo moieties; at the same time, selective reflection can be seen with outside pressing on heating and cooling cycles, but the absorption peak cannot be observed on the UV–Vis spectrum without pressing. Both P series and AP series exhibited optical activity and showed the same handedness as chiral cores. Moreover, the photoresponsive behaviors of the AP series polymers were also investigated. The direction rotation of AP changed with the increase in UV irradiation time. The X-ray diffraction analysis further approved that all the obtained polymers showed a cholesteric phase.

Compliance with ethical standards

Funding This study was funded by Fundamental Research Funds for the Central Universities (N130205001), The National Natural Science Foundation (51273035), and the Scientific and Technical Bureau Foundation of Shen Yang City (F16-205-1-03).

Conflict of interest The authors declare that they have no conflict of interest.

References

1. Natansohn A, Rochon P (2002) Photoinduced motions in azo-containing polymers. Chem Rev 102(11):4139–4175
2. Archut A, Azzellini GC, Balzani V, et al. (1998) Toward photoswitchable dendritic hosts. Interaction between azobenzene-functionalized dendrimers and eosin. J Am Chem So 120(47): 12187–12191
3. Jiang DL, Aida T (1997) Photoisomerization in dendrimers by harvesting of low-energy photons. Nature 388(6641):454–456
4. Lin PC, Cong YH, Sun C, Zhang BY (2016) Non-covalent modification of reduced graphene oxide by a chiral liquid crystalline surfactant. Nanoscale 8(4):2403–2411
5. Marin L, Zabulica A, Sava M (2011) New symmetric azomethinic dimer: the influence of structural heterogeneity on the liquid crystalline behaviour. Liq Cryst 38(4):433–440
6. Andruzzi L, D'Apollo F, Galli G, et al. (2001) Synthesis and structure characterization of liquid crystalline polyacrylates with unconventional fluoroalkylphenyl mesogens. Macromolecules 34(22): 7707–7714
7. Bobrovsky A, Shibaev V, Hamplova V, et al. (2016) Photo-optical properties of amorphous and crystalline films of azobenzene-containing photochromes with bent-shaped molecular structure. Photoch Photobio A 316:75–87
8. Bobrovsky A, Shibaev V, Bubnov A, et al. (2013) Effect of molecular structure on chiro-optical and photo-optical properties of smart liquid crystalline polyacrylates. Macromolecules 46(11):4276–4284
9. Ryabchun A, Bobrovsky A, Stumpe J, et al. (2015) Rotatable diffraction gratings based on cholesteric liquid crystals with phototunable helix pitch. Adv Opt Mater 3(9):1273–1279
10. Meng FB, He XZ, Zhang XD, et al. (2011) Effect of terminal perfluorocarbon chain containing mesogens on phase behaviors of chiral comb-like liquid crystalline polymers. Colloid Polym Sci 289(8):955–965
11. Han DH, Tong X, Zhao Y, et al. (2010) Cyclic azobenzene-containing side-chain liquid crystalline polymers: synthesis and topological effect on mesophase transition, order, and photoinduced birefringence. Macromolecules 43(8):3664–3671
12. Gimenez R, Millaruelo M, Pinol M, et al. (2005) Synthesis, thermal and optical properties of liquid crystalline terpolymers containing azobenzene and dye moieties. Polymer 46(22):9230–9242
13. Hattori H, Uryu T (2000) Synthesis and properties of photochromic liquid-crystalline copolymers containing both spironaphthoxazine and cholesteryl groups. J Polym Sci Pol Chem 38(5):887–894

14. Statman D, Basore V, Sulai Y, et al. (2008) Photoinduced gliding of the surface director in azo-dye doped nematic liquid crystals. Liq Cryst 35(1):33–38
15. Singh U, Davis F, Mohan S, Mitchell G (2013) Electro-active nanofibres electrospun from blends of poly-vinyl cinnamate and a cholesteric liquid crystalline silicone polymer. J Mater Sci 48(21): 7613–7619
16. Han M, Morino S, Ichimura K (2000) Factors affecting in-plane and out-of-plane photo orientation of azobenzene side chains attached to liquid crystalline polymers induced by irradiation with linearly polarized light. Macromolecules 33(17):6360–6371
17. Hvilsted S, Andruzzi F, Kulinna C, et al. (1995) Novel side-chain liquid-crystalline polyester architecture for reversible optical storage. Macromolecules 28(7):2172–2183
18. Apreutesei D, Mehl GH, Scutaru D (2007) Ferrocene-containing liquid crystals bearing a cholesteryl unit. Liq Cryst 34(7):819–831
19. Lin PC, Cong YH, Zhang BY (2015) Dispersing carbon nanotubes by chiral network surfactants. ACS Appl Mater Interfaces 7(12): 6724–6732
20. Agnieszka I, Boharewicz B, Tazbir I, et al. (2015) Laser beam induced current technique of polymer solar cells based on new poly(azomethine) or poly(3-hexylthiophene. Solid State Electron 104:53–63
21. Abrakhi S, Peralta S, Cantin S, et al. (2012) Synthesis and characterization of photosensitive cinnamate-modified cellulose acetate butyrate spin-coated or network derivatives. Colloid Polym Sci 290(5):423–434
22. Tejedor RM, Oriol L, Serrano J, et al. (2007) Photoinduced chiral nematic organization in an achiral glassy nematic azopolymer. Adv Funct Mater 17:3486–3492
23. Bobrovsky A, Shibaev V (2006) A study of photooptical processes in photosensitive cholesteric azobenzene-containing polymer mixture under an action of the polarized and nonpolarized light. Polymer 47(12):4310–4317
24. Andruzzi L, Altomare A, Ciardelli F, et al. (1999) Holographic gratings in azobenzene side-chain polymethacrylates. Macromolecules 32:448–454
25. Viswanathan NK, Kim DY, Bian S, et al. (1999) Surface relief structures on azo polymer films. J Mater Chem 9(9):1941–1955
26. Karim MR, Sheikh MRK, Yahya R, et al. (2015) Synthesis of polyme-rizable liquid crystalline monomers and their side chain liquid crystalline polymers bearing azo-ester linked benzothiazole mesogen. Colloid Polym Sci 293:1923–1935
27. Kanazawa A, Hirano S, Shishido A, et al. (1997) Photochemical phase transition behaviour of polymer azobenzene liquid crystals with flexible siloxane units as a side-chain spacer. Liq Cryst 23(2): 293–298
28. Jui-Hsiang L, Yang P-C, Wang Y-K, et al. (2006) Optical behaviour of cholesteric liquid crystal cells with novel photoisomerizable chiral dopants. Liq Cryst 33(3):237–248
29. Ho MS, Natansohn A, Rochon P (1996) Synthesis and optical properties of poly{(4-nitrophenyl)-[3-[N-[2-(methacryloyloxy)ethyl]-carbazolyol]]diazene}. Macromolecules 29(1):44–49
30. Zettsu N, Ogasawara T, Mizoshita N, et al. (2008) Photo-triggered surface relief grating formation in supramolecular liquid crystalline polymer systems with detachable azobenzene units. Adv Mater 20(3):516–521
31. Forcen P, Oriol L, Sanchez C, et al. (2007) Synthesis, characterization and photoinduction of optical anisotropy, in liquid crystalline diblock azo-copolymers. J Polym Sci Pol Chem 45(10):1899–1910
32. Bobrovsky A, Shibaev V, Hamplova V, et al. (2010) Gel formation and photoactive properties of azobenzene-containing polymer in liquid crystal mixture. Colloid Polym Sci 288:1375–1384
33. Srinivasan MV, Kannan P, Roy A (2013) Photo and electrically switchable behavior of azobenzene containing pendant bent-core liquid crystalline polymers. J Polym Sci Pol Chem 51:936–946
34. Yang ZQ, Herd GA, Clarke SM, et al. (2006) Thermal and UV shape shifting of surface topography. J Am Chem Soc 128:1074–1075
35. Delaire J, Nakatani K (2000) Linear and nonlinear optical properties of photochromic molecules and materials. Chem Rev 100: 1817–1846
36. Mahimwalla Z, Yager KG, Jun-ichi, et al. (2012) Azobenzene photomechanics: prospects and potential applications. Polym Bull 69:967–1006
37. Ana-Maria R, Luiza E, Nicolae H (2010) Surface properties, thermal behaviorand molecular simulation of azo-polysiloxanes under light stimuli. Insight into the relaxation. Macromol Res 18:721–729
38. Zhou QL, Yan SK, Han CC, et al. (2008) Promising functional materials based on ladder polysiloxanes. Adv Mater 20:2970–2976
39. Kaspar M, Bubnov A, Hamplova V, et al. (2004) New ferroelectric liquid crystalline materials with an azo group in the molecular core. Liq Crtyst 31(6):821–830
40. Cigl M, Fodor-Csorba K, et al. (2014) Functional photochromic methylhydrosiloxane -based side-chain liquid crystalline polymer. Macromol Chem Phys 215:742–752
41. Abe J, Hasegawa M, Matsushina H, et al. (1995) Investigation of dipolar alignment of mesogenic chromophores in side chain liquid crystalline polysiloxane using electric field induced second harmonic generation. Macromolecules 28(8):2938–2943